Maintenance of antiangiogenic and antitumor effects by orally active low-dose capecitabine for long-term cancer therapy

Yin Zhang[a,b,c,1], Meili Sun[b,d,1], Guichun Huang[b,1], Linlin Yin[b,e], Qinghua Lai[b,d], Yunlong Yang[b,f], Xiaoming Xing[a], Guohua Yu[g], Yuping Sun[d,2], Xinsheng Wang[a,2], Guohui Nie[f,2], Yizhi Liu[c,2], and Yihai Cao[a,b,c,f,2]

[a]Central Research Laboratory, The Affiliated Hospital of Qingdao University, Qingdao 266071, China; [b]Department of Microbiology, Tumor and Cell Biology, Karolinska Institute, 171 77 Stockholm, Sweden; [c]State Key Laboratory of Ophthalmology, Zhongshan Ophthalmic Center, Sun Yat-Sen University, Guangzhou 510060, China; [d]Department of Oncology, Jinan Central Hospital, Shandong University, Jinan, Shandong 250013, China; [e]Department of Hematology and Oncology, The Fourth Hospital of Jinan, Jinan, Shandong 250031, China; [f]Key Laboratory of International Collaborations, Second People's Hospital of Shenzhen, First Affiliated Hospital of Shenzhen University, Shenzhen 518035, China; and [g]Department of Oncology, Wei Fang People's Hospital, Weifang, Shandong 261041, China

Edited by Robert Langer, MIT, Cambridge, MA, and approved May 15, 2017 (received for review March 29, 2017)

Long-term uninterrupted therapy is essential for maximizing clinical benefits of antiangiogenic drugs (AADs) in cancer patients. Unfortunately, nearly all clinically available AADs are delivered to cancer patients using disrupted regimens. We aim to develop lifetime, nontoxic, effective, orally active, and low-cost antiangiogenic and antitumor drugs for treatment of cancer patients. Here we report our findings of long-term maintenance therapy with orally active, nontoxic, low cost antiangiogenic chemotherapeutics for effective cancer treatment. In a sequential treatment regimen, robust antiangiogenic effects in tumors were achieved with an anti-VEGF drug, followed by a low-dose chemotherapy. The nontoxic, low dose of the orally active prodrug capecitabine was able to sustain the anti-VEGF–induced vessel regression for long periods. In another experimental setting, maintenance of low-dose capecitabine produced greater antiangiogenic and antitumor effects after AAD plus chemotherapy. No obvious adverse effects were developed after more than 2-mo of consecutive treatment with a low dose of capecitabine. Together, our findings provide a rationalized concept of effective cancer therapy by long-term maintenance of AAD-triggered antiangiogenic effects with orally active, nontoxic, low-cost, clinically available chemotherapeutics.

angiogenesis | VEGF | tumor growth | cancer therapy | chemotherapy

The concept of angiogenesis-dependent tumor growth and blocking tumor blood vessel growth for cancer therapy remains an undisputed dogma (1, 2). To stimulate new vessel growth, tumors produce numerous angiogenic proteins that are often categorized as angiogenic factors and cytokines (3–6). Consequently, blocking the functions of these tumor-produced angiogenic factors provides an outstanding opportunity for cancer therapy (3, 7). Among tumor-derived angiogenic factors, vascular endothelial growth factor (VEGF) is probably the best-characterized angiogenic protein that activates its endothelial cell receptors, i.e., VEGFR1 and VEGFR2, triggering distinct signaling pathways (8–10). VEGF displays broad biological functions on endothelial cells and nonvascular cells including but not limited to angiogenesis, vascular permeability, hematopoiesis, vascular survival, vasculogenesis, metabolism, inflammation, neurogenesis, vascular remodeling, and endocrine functions (11). In addition to inhibition of tumor vasculatures, blocking VEGF functions would have broad functional impacts on multiple tissues and organs (12–15).

Almost all Food and Drug Administration (FDA)-approved antiangiogenic drugs (AADs) contain an anti-VEGF component, and targeting VEGF and its receptor signaling has become a swarming area for anticancer drug development (2, 7, 11, 16). In experimental animal models, anti-VEGF monotherapy shows potent antiangiogenic and antitumor effects (17). However, AAD monotherapy is generally ineffective or produces only modest beneficial effects in most clinical trials (2, 16). Combination of AAD with chemotherapy demonstrates improvement of survival benefits and is the most commonly used regimen for treatment of most cancer types (18–20). To maximize AAD clinical benefits, one of the key unresolved issues is to achieve nonstop lifetime therapy in cancer patients because discontinuation of AAD treatment can cause a rebound effect of tumor neovascularization (21–24). Additionally, withdrawal of AADs might promote cancer metastasis through a vascular recovery mechanism in remote tissues and organs (13). Several clinical trials show that prolonged AAD therapy increases survival benefits in cancer patients (25–27). Owing to lack of obvious benefits, development of adverse effects, and high cost issues, withdrawal of antiangiogenic therapy inevitably occurs in almost all cancer patients. In fact, the currently approved therapeutic regimen itself employs drug holidays for treatment of cancer patients. Recent work shows that withdrawal of AADs results in a rapid rebound neovascularization in tumors and causes potential metastasis in preclinical models (13, 15, 28). Thus, long-term incessant therapy is needed for maximizing clinical benefits.

Nondisrupted long-term maintenance therapy is a highly challenging issue, demanding negligible side effects, convenient delivery, and low affordable cost of a drug. In this work, we show that capecitabine as an orally active chemotherapeutic drug with

Significance

Withdrawal of antiangiogenic drugs leads to tumor revascularization, even rebound effects of tumor angiogenesis, and potential metastasis. Long-term maintenance therapy with antiangiogenic drugs is crucial for achieving maximal clinical benefits for cancer patients. There are no antiangiogenic drugs that are clinically available for maintenance therapy. We show that orally active capecitabine at an extremely low and nontoxic dose displays a potent antiangiogenic effect that can be used for maintenance therapy. Importantly, the low-dose capecitabine in a sequentially therapeutic setting following anti-VEGF drugs produces remarkable anticancer effects. If successfully proven in clinical settings, our therapeutic regimen would be beneficial for millions of cancer patients. Our findings will shift the paradigm of current antiangiogenic therapy for treatment of human cancer patients.

Author contributions: Y.C. designed research; Y.Z., M.S., G.H., L.Y., Q.L., and Y.Y. performed research; Y.Y., X.X., G.Y., Y.S., X.W., G.N., and Y.L. contributed new reagents/analytic tools; Y.Z. and Y.C. analyzed data; and Y.C. wrote the paper.

The authors declare no conflict of interest.

This article is a PNAS Direct Submission.

[1]Y.Z., M.S., and G.H. contributed equally to this work.

[2]To whom correspondence may be addressed. Email: 13370582181@163.com, qdfywxs@163.com, nghui@21cn.com, yizhi_liu@yahoo.com, or yihai.cao@ki.se.

This article contains supporting information online at www.pnas.org/lookup/suppl/doi:10.1073/pnas.1705066114/-/DCSupplemental.

www.pnas.org/cgi/doi/10.1073/pnas.1705066114

potent antiangiogenic activity can be used at an extremely low and nontoxic dose to sustain anti-VEGF effects in tumors. In a sequential drug delivery setting, the low-dose capecitabine produces similar antiangiogenic and antitumor effects as an anti-VEGF neutralizing antibody. Based on our findings, we propose a concept of sequential therapy, i.e., anti-VEGF treatment followed by a low dose schedule of capecitabine.

Results

Identification of 5-FU as a Potent Endothelial Cell Inhibitor. Our initial idea of developing AAD maintenance therapy was to identify an FDA-approved cancer drug that could be used immediately in the clinic. For this purpose, we screened different classes of chemotherapeutics for their ability to inhibit endothelial cell and tumor cell proliferation. These chemotherapeutics included antimetabolites, DNA alkylating agents, antibiotics, and plant alkaloids (Fig. 1). We used capillary endothelial cells for proliferation assay because these microvascular endothelial cells would recapitulate those in the tumor microenvironment. Among antimetabolites, 5-FU showed a potent effect on inhibition of capillary endothelial cell growth (Fig. 1*A*). IC_{50} of 5-FU on endothelial cell proliferation was about 2.0 μM, whereas human squamous cell carcinoma, colorectal cancer, and breast cancer cells were less sensitive or insensitive. These findings demonstrate that 5-FU preferentially inhibits endothelial cell proliferation if tumor cells and endothelial cells coexist.

Gemcitabine and pemetrexed, two other antimetabolites, did not show a preferably inhibitory effect on endothelial cells. In contrast, tumor cells appeared to be more sensitive than endothelial cells in response to these two drugs (Fig. 1*A*). Similarly, alkylating agents (cisplatin and oxaliplatin), antibiotic (doxorubicin), and plant alkaloids (paclitaxel, docetaxel, and vinorelbine) did not show preferable inhibition of endothelial cell growth relative to tumor cells (Fig. 1 *B*–*D*). These data show that 5-FU is a preferable inhibitor for endothelial cells.

5-FU as a Preferential Inhibitor for Endothelial Cells. Knowing that 5-FU is a potent endothelial cell inhibitor, we further studied its inhibitory effects on endothelial cells in comparison with tumor cells. In a 3-(4,5-dimethylthiazol-2-yl)-2,5-diphenyltetrazolium bromide (MTT)–based cell proliferation assay, 5-FU showed potent inhibitory effects on proliferation of capillary endothelial cells (CECs) at concentrations ranging from 1.2 μM to 19.1 μM (Fig. 2*A*). By contrast, 5-FU only demonstrated inhibitory effects on colorectal cancer (CRC) cell proliferation at high concentrations, i.e., 9.6 μM and 19.1 μM, and did not exhibited any significant inhibitory effects at low concentrations (Fig. 2*A*). Similar to CECs, 5-FU also potently inhibited human endothelial cell [human umbilical vein endothelial cell (HUVEC)] proliferation at 2.4 μM, which showed no effect on human CRC cells (Fig. 2*B*). Although at high concentrations 5-FU also inhibited human CRC cell proliferation, the magnitude of the inhibitory effect on HUVECs was greater than on tumor cells.

Consistent with its inhibitory effects of cell proliferation, 5-FU also significantly decreased the $Ki67^+$ cell population in CECs. The inhibitory effects on endothelial cells were markedly greater than those on CRC tumor cells (Fig. 2 *C* and *D*). As for HUVECs, low concentrations of 5-FU displayed potent inhibitory effects, whereas human CRC cells showed resistance to 5-FU treatment (Fig. 2*D*). 5-FU also potently induced endothelial cell apoptosis, whereas CRC tumor cells showed intrinsic resistance to cellular apoptosis even at high concentrations (Fig. 2 *E* and *F*). These findings demonstrate that 5-FU preferentially inhibits endothelial cell proliferation relative to tumor cells.

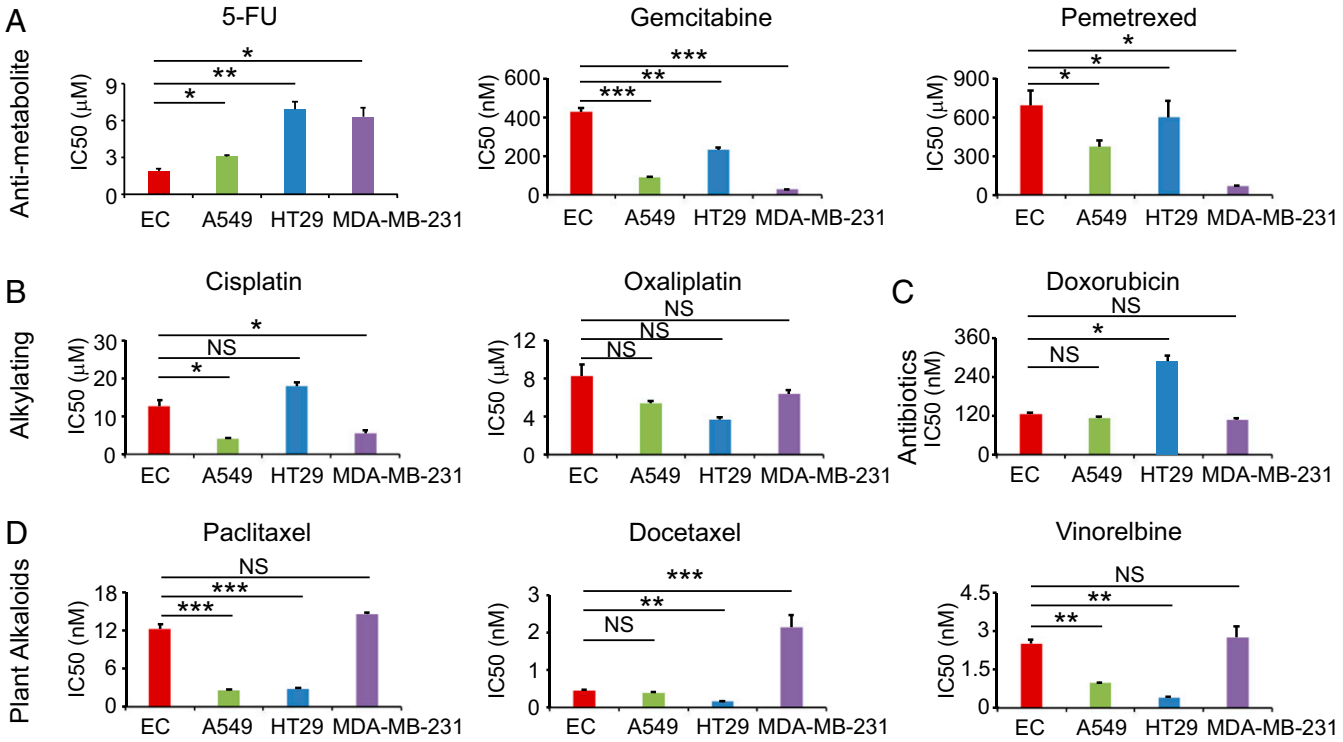

Fig. 1. Antiproliferative effects of chemotherapeutics. IC_{50} values of a MTT assay were used to determine the antiproliferative effect. EC: endothelial cell; A549: human lung carcinoma; HT29: human colorectal adenocarcinoma; MDA-MB-231: human breast adenocarcinoma. (*A*) Inhibitory effects by antimetabolite drugs. (*B*) Inhibitory effects by alkylating drugs. (*C*) Inhibitory effects by cytostatic antibiotics. (*D*) Inhibitory effects by plant alkaloids. Data were quantified as mean determinants ($n = 3$ samples per group). Each experiment was repeated at least twice. Data are means ± SEM. $^*P < 0.05$; $^{**}P < 0.01$; $^{***}P < 0.001$. NS, not significant.

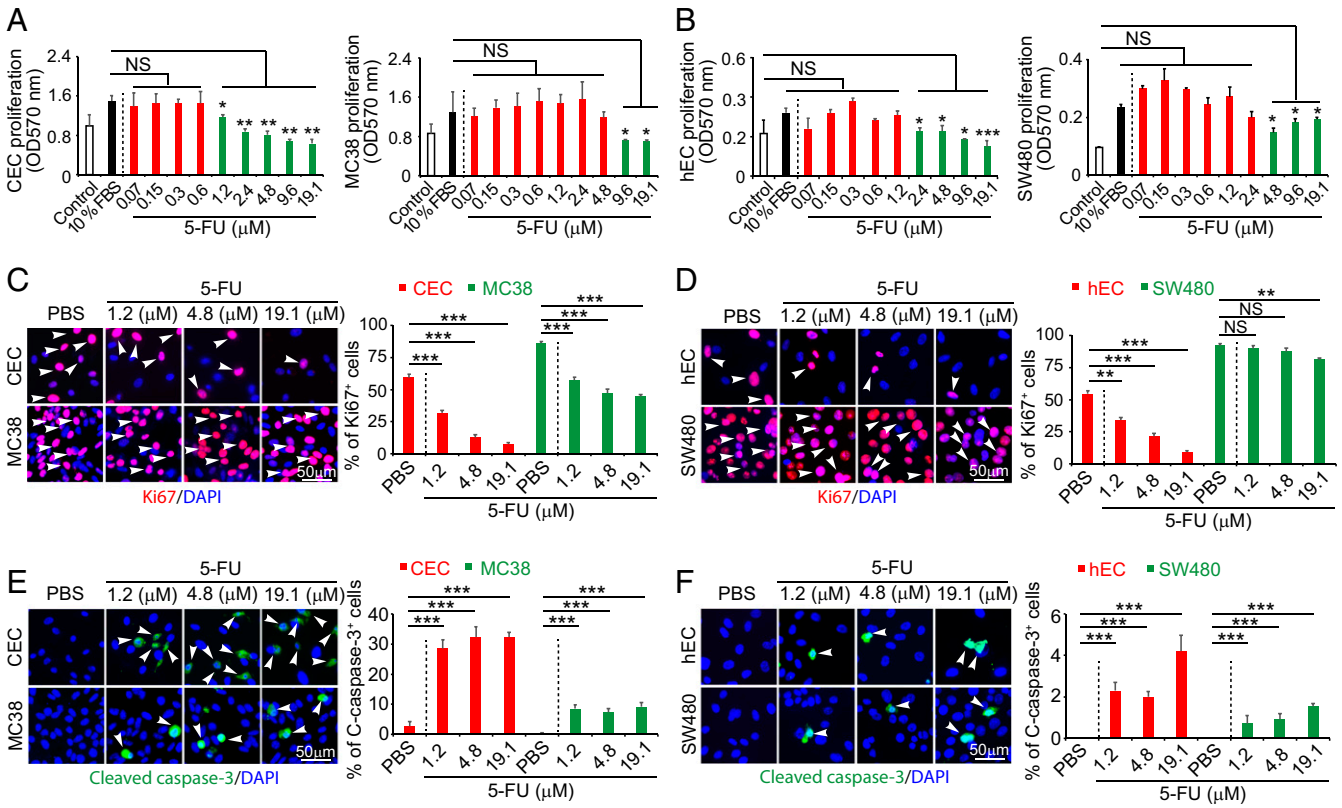

Fig. 2. In vitro inhibitory effects of 5-FU on cell proliferation. (*A* and *B*) Inhibition of animal (CEC and MC38) and human (hEC and SW480) endothelial cell and colorectal cancer proliferation by various concentrations of 5-FU ($n = 3$ samples per group). (*C* and *D*) Antiproliferative effects of various concentrations of 5-FU on animal and human ECs and CRCs ($n = 3$ samples per group). Arrowheads indicate Ki67$^+$ proliferating cells. (*E* and *F*) Induction of apoptosis by various concentrations of 5-FU on animal and human ECs and CRCs ($n = 3$ samples per group). Arrowheads indicate cleaved caspase 3$^+$ apoptotic cells. Data are means ± SEM. $^{**}P < 0.01$; $^{***}P < 0.001$. NS, not significant.

Antiangiogenic and Antitumor Effects of 5-FU. We next studied the antiangiogenic and antitumor effects of 5-FU in a mouse CRC model. In this experimental setting, 5-FU treatment at various dosages was initiated when a tumor reached the size of ~0.2 cm^3. A dose-dependent inhibition of tumor growth was seen in this mouse tumor model (Fig. 3*A*). At 2.5 mg/kg, 5-FU showed a trend, but statistically insignificant, inhibition of tumor growth. At the dose of 25 mg/kg, 5-FU completely blocked tumor growth (Fig. 3*A*). Similar to antitumor activity, 5-FU also demonstrated a dose-dependent antiangiogenic effect by decreasing microvessel density (Fig. 3 *B* and *C*). The degree of vascular reduction was well correlated with the antitumor effects. Consistent with decreases of vascular density, increases of 5-FU dosages also led to higher degrees of tumor tissue hypoxia (Fig. 3 *B* and *D*). Along with increased antitumor activity, a dose-dependent inhibition of tumor cell proliferation and increased cellular apoptosis were also detectable in immunohistochemical sections (Fig. 3 *B*, *E*, and *F*). These findings demonstrate that 5-FU monotherapy potently inhibited tumor angiogenesis, leading to attenuated tumor growth, elevation of hypoxia, and increase of cellular apoptosis in an in vivo CRC tumor model. Despite its potent antiangiogenic and antitumor effects, 5-FU at low doses did not significantly inhibit hematopoiesis, hepatic function, or kidney function (Fig. S1).

Anti-VEGF and 5-FU Sequential Therapy. Given the potent antiangiogenic effect of 5-FU, we hypothesized that 5-FU might be used as an antiangiogenic maintenance drug followed by anti-VEGF therapy. To prove this concept, we used 5-FU for the initial tumor studies. In this sequential experimental setting, we aimed to sustain the anti-VEGF–induced antiangiogenic effect by 5-FU (Fig. 4*A*). Tumors were treated with VEGF blockade for 1 wk, subsequently switching to a low-dose (5 mg/kg) 5-FU for 18 d. Expectedly, anti-VEGF treatment alone produced robust antitumoral and antiangiogenic effects in this CRC tumor model (Fig. 4 *B*–*D*). Withdrawal of anti-VEGF treatment resulted in a rapid revascularization in tumors, restoring tumor growth (Fig. 4 *B*–*D*). Despite the long half-life of the anti-VEGF antibody, microvessel density in off-drug anti-VEGF tumors was completely recovered to the level of the control nonimmune IgG-treated tumors. However, in the sequential anti-VEGF/5-FU–treated group, tumors remained in their smaller sizes throughout the experimental duration (Fig. 4*B*). Importantly, after the initial anti-VEGF treatment for 1 wk, switching to continuous anti-VEGF or a low-dose 5-FU did not produce any difference in terms of the antitumor effects (Fig. 4*B*). These data demonstrate that the low-dose 5-FU is as effective as VEGF blockade in sustaining the VEGF-triggered antitumor effects. Consistent with the impaired tumor growth, the sequential anti-VEGF/5-FU–treated tumors contained significantly fewer microvessels, which were equivalent to those of anti-VEGF–treated tumors (Fig. 4 *C* and *D*). Consistent with reduction of vascular density, sequential anti-VEGF/5-FU–treated tumors also experienced elevated tissue hypoxia (Fig. 4 *C* and *E*). The number of proliferating tumor cells was markedly decreased in the sequentially treated tumors (Fig. 4 *C* and *F*). By contrast, tumor cell apoptosis was markedly increased in sequential anti-VEGF/5-FU–treated tumors (Fig. 4 *C* and *G*). These data suggest the possibility of using 5-FU for long-term maintenance of antiangiogenic treatment.

Antiangiogenic and Antitumor Effects of Orally Active Capecitabine. For long-term maintenance therapy, an ideal antiangiogenic drug

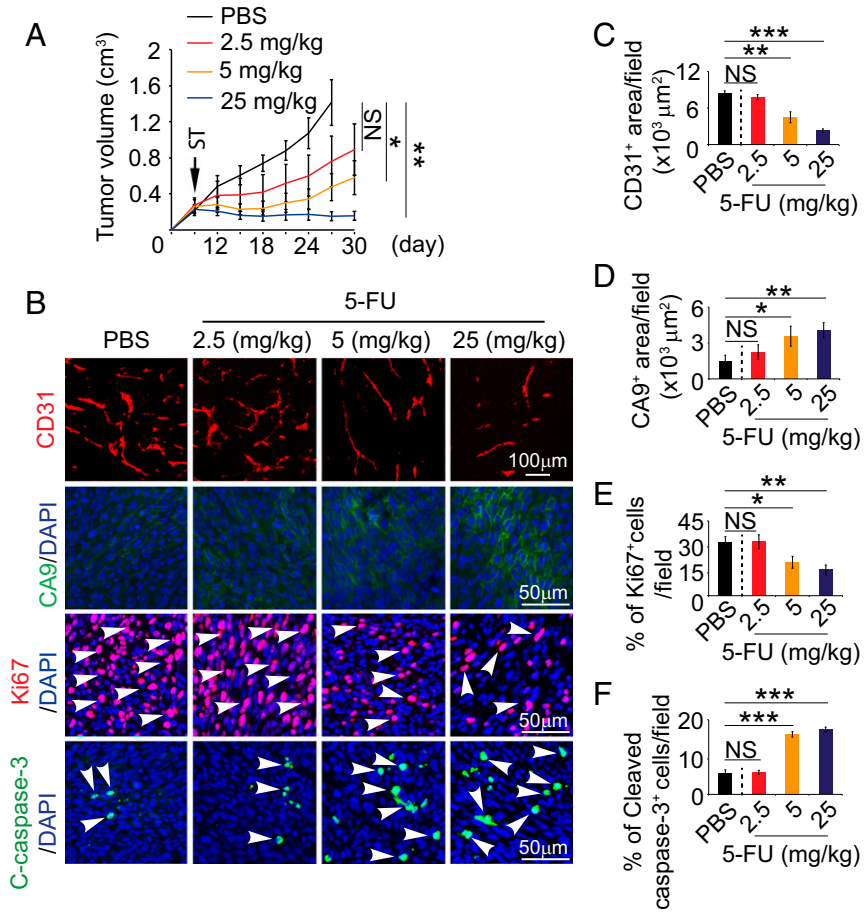

Fig. 3. 5-FU exhibits dose-dependent antitumor and antiangiogenic effects. (*A*) Growth rates of 5-FU–treated tumors (n = 6–8 animals per group). ST: starting treatment. (*B*) Representative histological images of CD31$^+$ blood vessels, CA9$^+$ hypoxia, Ki67$^+$ proliferating cells, and cleaved caspase-3$^+$ apoptotic cells. Arrowheads point to proliferating (red signal) and apoptotic (green signal) cells. (*C*–*F*) Quantifications of CD31$^+$ blood vessels, CA9$^+$ hypoxia, Ki67$^+$ proliferating cells, and cleaved caspase-3$^+$ apoptotic cells in 5-FU–treated tumors (n = 6–8 random fields per group). Data are means ± SEM. *P < 0.05; **P < 0.01. ***P < 0.001. NS, not significant.

should fulfill several rigorous criteria for clinical use. These include low toxicity, convenient administration, low cost, and availability in the market. For these reasons, we further studied the orally active capecitabine, a prodrug for 5-FU, for its ability to suppress tumor angiogenesis. Especially, we were interested in investigating the impact of low doses of capecitabine on tumor angiogenesis. First, a dose-escalation effect of capecitabine was tested on tumor growth and angiogenesis. We used the clinical equivalent dose, i.e., 500 mg/kg, as the maximal dose and lower doses ranging from 250 mg/kg to 31 mg/kg. The minimal dose at 31 mg/kg was 16-fold lower than the clinically used dose. First, we assessed the toxicity of these dosages in CRC tumor-bearing mice. Except for the highest dose of 500 mg/kg, all doses did not produce any overt adverse effects over 3 wk. All low dosages (lower than the standard clinical dose) had no impacts on body weight, food intake, white blood cell count, red blood cell count, platelet numbers, serum albumin levels, serum alanine aminotransferase (ALT) levels, aspartate aminotransferase (AST), blood urea nitrogen, or serum creatinine (Fig. S2). Thus, hematopoiesis, liver function, and kidney function were not affected by low doses of capecitabine.

Surprisingly, dosages spanning over this maximal–minimal range produced similar antitumor effects in our CRC model (Fig. 5*A*). The antitumor effects of these various dosages of capecitabine were statistically indistinguishable, although higher dosages had a trend of increased antitumor activity. Consistently, capecitabine at all doses demonstrated potent antiangiogenic effects, which were statistically insignificant among various groups (Fig. 5 *B* and *C*). More than 60% reduction of vascular density was found in various dose-treated tumors relative to control tumors (Fig. 5*B*). Also, numbers of proliferating tumor cells were markedly decreased in capecitabine-treated tumors at all doses (Fig. 5 *B* and *D*). Conversely, cellular apoptosis was significantly increased upon capecitabine treatment (Fig. 5 *B* and *E*). These findings demonstrate that capecitabine is an orally active potent antiangiogenic chemotherapeutic drug.

Antiangiogenic Maintenance Therapy by Capecitabine. To investigate the antiangiogenic maintenance effect of capecitabine, we designed a sequential therapeutic regimen in which a CRC tumor was treated with VEGF blockade for 7 d, followed by the lowest dose (16-fold lower than the standard clinical dose) of capecitabine for more than 30 d (Fig. 6*A*). We included both negative and positive controls in this experimental setting (Fig. 6*A*). As expected, uninterrupted treatment with VEGF blockade produced a marked antitumor effect relative to the nonimmune IgG isotype (NIIgG)-treated group (Fig. 6*B*). Interestingly, continuous treatment with the lowest dose of capecitabine produced a nearly identical antitumor effect as seen with VEGF blockade (Fig. 6*B*). In an anti-VEGF off-drug setting, drug withdrawal after 1 wk of VEGF blockade did not show any significant antitumor activity compared with the NIIgG-treated

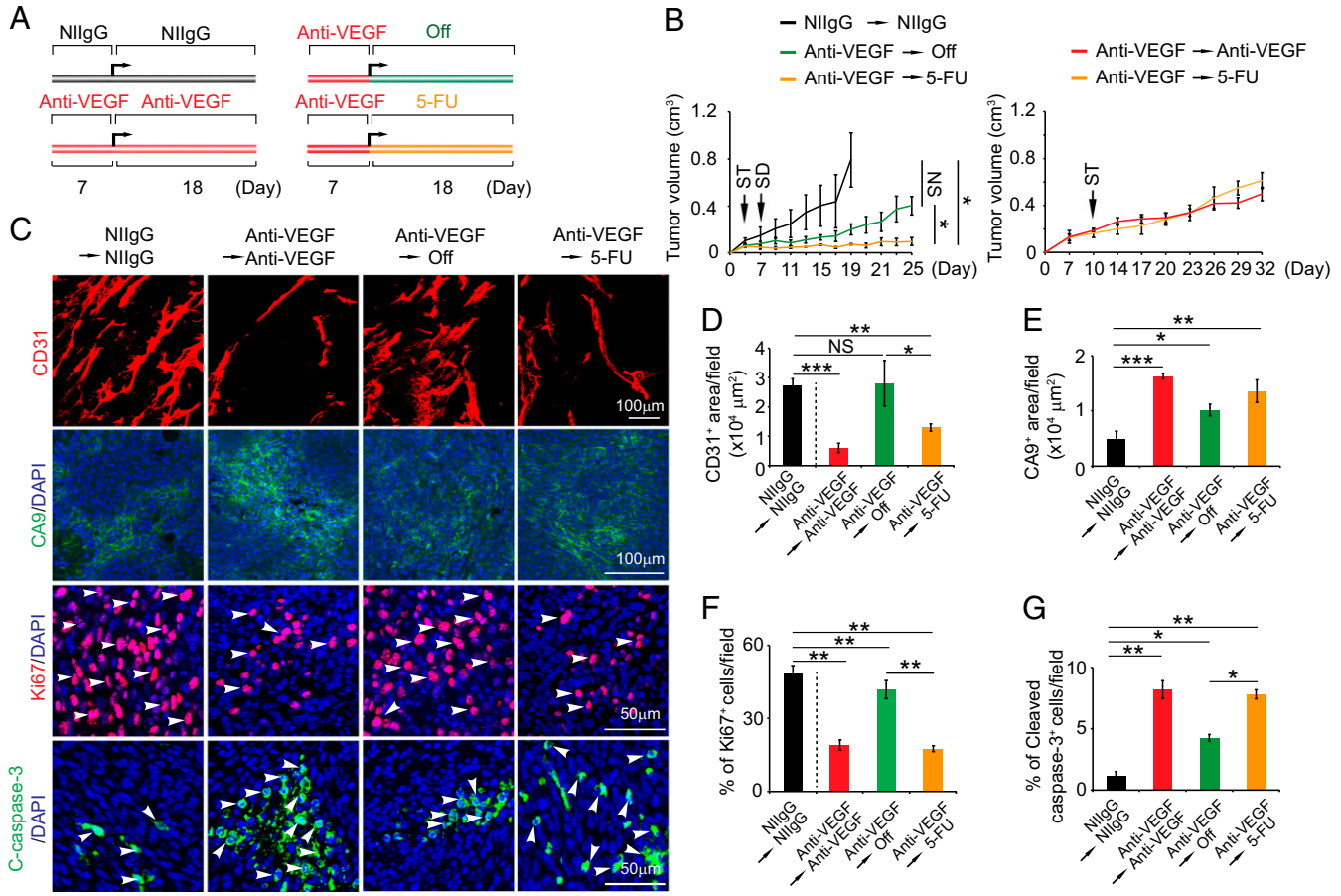

Fig. 4. 5-FU–induced antiangiogenic maintenance in colorectal tumors. (*A*) Treatment schedule. (*B*) Growth rates of continuous NIIgG-treated, continuous VEGF blockade-treated, VEGF blockade and cessation-treated, and VEGF blockade followed by a low dose of 5-FU–treated MC38 colorectal cancers (n = 6–7 mice per group). ST: starting treatment; SD: switching drug. (*C*) Representative histological images of CD31$^+$ blood vessels, CA9$^+$ hypoxia, Ki67$^+$ proliferating cells, and cleaved caspase-3$^+$ apoptotic cells. Arrowheads point to proliferating (red signal) and apoptotic (green signal) cells. (*D*–*G*) Quantifications of CD31$^+$ blood vessels, CA9$^+$ hypoxia, Ki67$^+$ proliferating cells, and cleaved caspase-3$^+$ apoptotic cells in various agent-treated tumors (n = 6–8 random fields per group). Data are means ± SEM. *P < 0.05; **P < 0.01. ***P < 0.001. NS, not significant.

group (Fig. 6*B*). These data support the notion of noninterrupted long-term anti-VEGF treatment for sustaining its antitumor effect. These findings also indicate that tumors restore their growth capacity immediately upon cessation of anti-VEGF treatment despite anti-VEGF antibody's long half-life in the body. Importantly, termination of anti-VEGF therapy followed by the low dose of capecitabine sustained the anti-VEGF–initiated antitumor effect (Fig. 6*B*). Thus, capecitabine was able to maintain the anti-VEGF–triggered antitumor activity in our experimental models.

Along with the antitumor activity, switching VEGF blockade to the low dose of capecitabine completely sustained the angiostatic effect of VEGF blockade (Fig. 6 *C* and *D*). Similarly, capecitabine alone at the low dose also produced a potent antiangiogenic effect. Blood perfusion and vascular permeability were significantly inhibited in continuous anti-VEGF–, continuous capacitabine-, and sequential anti-VEGF/capecitabin-treated tumors (Fig. S3). Tumor tissues also experienced increased hypoxia in the treated groups (Fig. S3). Tumor cell proliferation and cellular apoptosis in these treated groups were significantly inhibited and increased, respectively (Fig. 6 *C*, *E*, and *F*). Together, these data show that capecitabine at a nontoxic low dose is capable of maintaining anti-VEGF–initiated antiangiogenic and antitumor effects.

Long-Term Maintenance of Antitumor and Antiangiogenic Effects by a Low Dose of Capecitabine. During clinical practice, combinations of bevacizumab and chemotherapy are often simultaneously given to cancer patients. To recapitulate the clinical situation, we designed a regimen in which VEGF blockade and chemotherapy were simultaneously used for treating tumor-bearing mice for 2 wk (similar regimen approved for clinical use) (18). After 2-wk of combination therapy, the treatment was switched to the extremely low-dose capecitabine (16-fold lower than the clinical dose) alone for more than 6 wk (Fig. 7*A*). NIIgG-treated and VEGF blockade-treated followed by capecitabine served as controls. The NIIgG-treated tumors grew at an accelerated rate and reached nearly 1.2 cm^3 within 6 wk (Fig. 7*B*). Similarly, cessation of anti-VEGF plus capecitabine also resulted in restoration of an accelerated tumor growth rate (Fig. 7*B*), indicating that combination therapy was unable to sustain the long-term antitumor activity. By contrast, maintenance with the low dose of capecitabine alone after withdrawal of VEGF blockade plus capecitabine produced marked antitumor effect (Fig. 7*B*). Tumors in this group remained at smaller sizes without further growth for more than 2 mo, and some tumors even showed regression (Fig. 7*B*). Similarly, low-dose capecitabine maintenance after withdrawal of VEGF blockade also produced remarkable long-term antitumor activity (Fig. 7*B*). These data demonstrate that oral administration of the low dose of capecitabine after cessation of VEGF blockade or combination of VEGF blockade plus capecitabine produces long-term and potent antitumor activity.

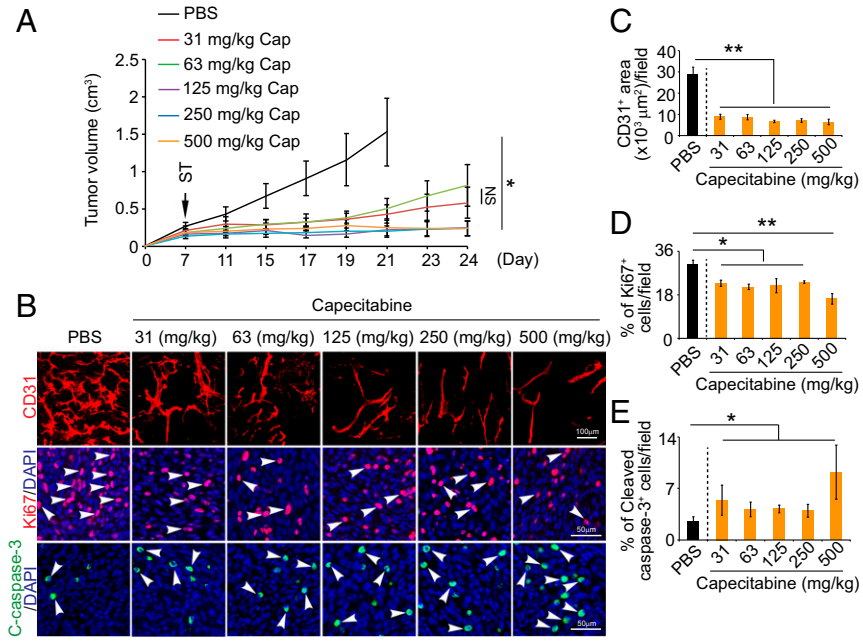

Fig. 5. Dose-dependent antitumor and antiangiogenic effects by capecitabine. (*A*) Growth rates of capecitabine (Cap)-treated tumors (n = 6–8 animals per group). ST: starting treatment. (*B*) Representative histological images of CD31$^+$ blood vessels, Ki67$^+$ proliferating cells, and cleaved caspase-3$^+$ apoptotic cells. Arrowheads point to proliferating (red signal) and apoptotic (green signal) cells. (*C*–*E*) Quantifications of CD31$^+$ blood vessels, Ki67$^+$ proliferating cells, and cleaved caspase-3$^+$ apoptotic cells in 5-FU–treated tumors (n = 6–8 random fields per group). Data are means ± SEM. *P < 0.05; **P < 0.01. NS, not significant.

After a 2-wk treatment, VEGF blockade and combination of VEGF blockade plus capecitabine showed potent antiangiogenic effects in tumor tissues (Fig. S4). Interestingly, combination of VEGF blockade plus capecitabine produced a greater antiangiogenic effect than anti-VEGF treatment alone (Fig. S4), suggesting that anti-VEGF and capecitabine display an additive antiangiogenic effect and inhibit angiogenesis through different mechanisms. Along with inhibition of tumor angiogenesis, marked decreases of tumor cell proliferation and increases of cellular apoptosis and tumor hypoxia were also found in the anti-VEGF–treated and anti-VEGF plus capecitabine-treated tumor tissues (Fig. S4). Concordant with the antitumor effects, examination of tumor tissues at 67 d after maintenance therapy with capecitabine at the low dose after withdrawal of the anti-VEGF drug or combination therapy also produced potent antiangiogenic and antiproliferative effects (Fig. 7 *C*–*E*). Conversely, tumor cell apoptosis and hypoxia were markedly increased in capecitabine maintenance-treated tumors (Fig. 7 *B*, *F*, and *G*). Together, these data show that oral administration of an extremely low dose of capecitabine is able to maintain anti-VEGF drug-triggered antiangiogenic activity in tumors.

Discussion

Survival improvements by AADs in cancer patients either in monotherapy or combination therapeutic settings are rather limited (16). Clinically modest beneficial effects have raised many issues to challenge the original concept of antiangiogenic cancer therapy. These include the following: Do we use the appropriate AADs for treatment of human cancers? Are AAD targets suitable for all cancers? Have AADs been used for treatment of the subpopulation of responders of cancer patients? Are any biomarkers available to predict therapeutic benefits? How should the AAD resistance be circumvented? And, how long should cancer patients be treated? These are open questions for both basic scientists and clinical oncologists and are challenging for clinical practice. At this time of writing, these clinical issues remain unresolved. In the present work, we focus our efforts on developing a long-term nonstop antiangiogenic treatment for cancer patients.

Unlike most other cancer drugs that aim to eliminate malignant cells, the rationale of AADs is to suppress new blood vessel growth rather than to directly target tumor cells. Cessation of antiangiogenic therapy would inevitably reinitiate neovascularization and eventually tumor growth. In fact, in preclinical models withdrawal of antiangiogenic therapy results in rapid tumor revascularization and even a rebound phase of vessel growth (28), although off-drug–triggered rebound angiogenesis needs validation in human patients. Another surprising finding shows that cessation of antiangiogenic therapy could promote cancer metastasis owing to revascularization in nontumor tissues (13). Similar to tumor vasculatures, systemic delivery of AADs also induces vessel regression in nontumor tissues such as liver and endocrine organs (12–15). Intravasation and extravasation mechanisms are involved in facilitating cancer cells across the primitive vessel wall of growing vasculatures. Thus, AAD cessation-triggered detrimental effects are actually more overwhelming than what we originally thought.

Taking into consideration the off-drug–triggered devastating consequence, nonstop lifetime antiangiogenic therapy should be suggested for all cancer patients who receive AAD treatment. Would lifetime therapy be realistic for human cancer patients? The first unmet impediment is the cost issue. As these drugs are expensive and are not covered by healthcare in most parts of the world, it is almost impossible for patients to receive lifetime therapy. Also, when drug resistance occurs, patients are often advised to stop treatment. Similarly, development of AAD-associated adverse effects would often result in termination of therapy or taking off-drug holidays. In fact, the AAD treatment regimen itself lacks scientific rationale and employs "on" and "off" scheduling. As the process of off-AAD–initiated revascularization occurs quickly (28), off-drug holidays should be carefully considered. Along the line of our proposed lifetime therapy, several clinical trials have shown increased clinical benefits after prolonged antiangiogenic treatment (3, 19, 25, 26).

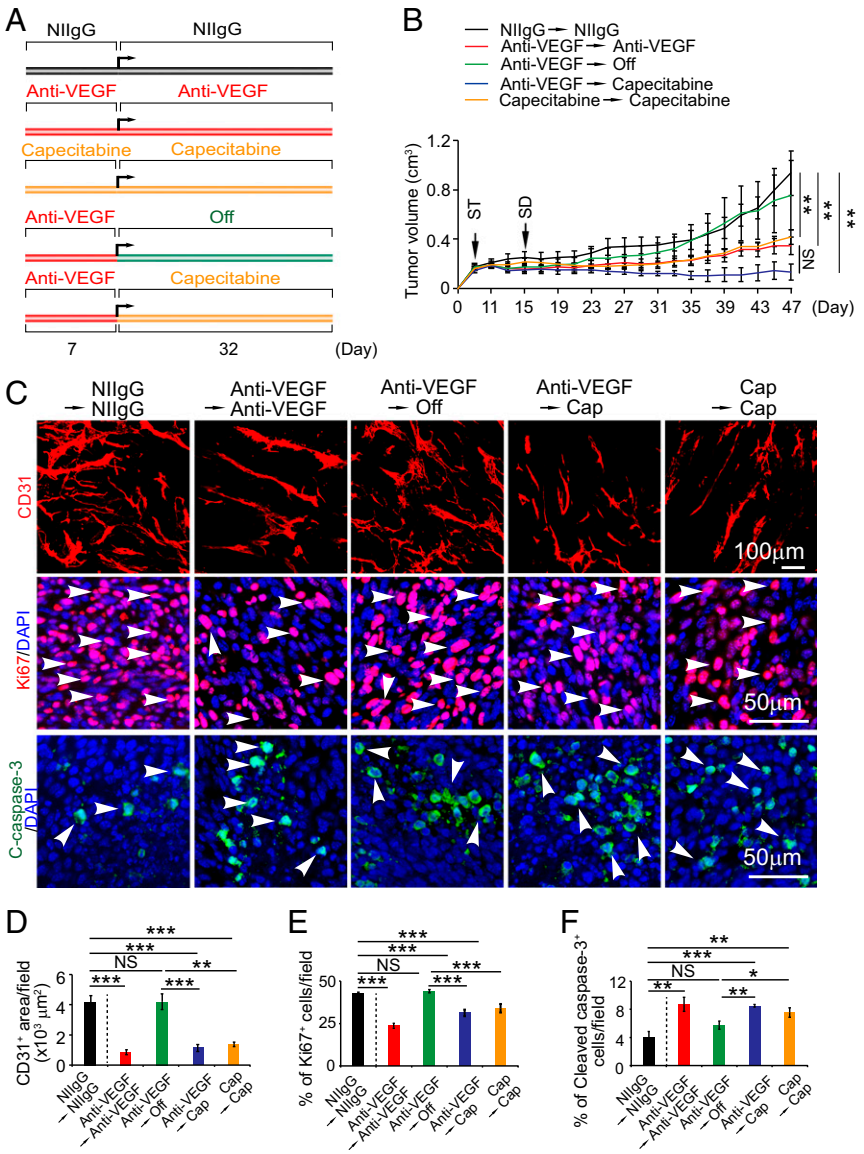

Fig. 6. Antiangiogenic and antitumor maintenance therapy with an extremely low dose of capecitabine. (*A*) Sequential treatment schedule. (*B*) Growth rates of continuous NIIgG-treated, continuous VEGF blockade-treated, continuous capecitabine-treated, VEGF blockade and cessation-treated, and VEGF blockade switching to low-dose capecitabine-treated MC38 colorectal cancers (n = 6–7 mice per group). ST: starting treatment; SD: switching drug. (*C*) Representative histological images of CD31$^+$ blood vessels, Ki67$^+$ proliferating cells, and cleaved caspase-3$^+$ apoptotic cells. Arrowheads point to proliferating (red signal) and apoptotic (green signal) cells. (*D–F*) Quantifications of CD31$^+$ blood vessels, Ki67$^+$ proliferating cells, and cleaved caspase-3$^+$ apoptotic cells in various agent-treated tumors (n = 6–8 random fields per group). Data are means ± SEM. *P < 0.05; **P < 0.01; ***P < 0.001. NS, not significant.

To achieve nonstop long-term antiangiogenic therapy, AADs should not produce overt toxicity; the cost should be sufficiently low and affordable by most, if not all, patients, and the delivery route should be convenient, ideally via orally available AADs. To fulfill these important criteria that meet clinical practice, we screened a broad spectrum of chemotherapeutics for assessing their antiangiogenic capacities. The rationale for screening chemotherapeutics is their clinical availability and because these drugs are used in combination with AADs in human patients. Despite antiproliferation as a common mode of action, various chemotherapeutics show tremendous variability for inhibition of endothelial cell growth. We have identified 5-FU as being the most potent chemotherapeutic for suppressing endothelial cell growth. In fact, both human and animal endothelial cells display higher sensitivity than proliferating tumor cells toward 5-FU treatment. Orally active capecitabine, as a prodrug for 5-FU, demonstrated potent antiangiogenic effects in animal tumor models. Although the mechanisms underlying the differential 5-FU responses between proliferating endothelial cells and cancer cells are not fully understood, it is highly plausible that different metabolic pathways in endothelial cells and cancers are responsible for specific targeting in endothelial cells. For example, cancer cells preferentially use glucose as the source of energy production; i.e., the Warburg effect and endothelial cells use a Warburg-independent metabolic pathway. It has been shown that antimetabolites down-regulate c-myc (29–31). In the sequential drug delivery settings, oral administration of a nontoxic low dose of capecitabine following AAD cessation sustained anti-VEGF drug-initiated antiangiogenic effects (Fig. 7*H*). The only possible problem for long-term therapy is that cancer cells might develop resistance toward capecitabine. However, the low dose of capecitabine is aimed to target endothelial cells rather than tumor cells. Another possible issue for

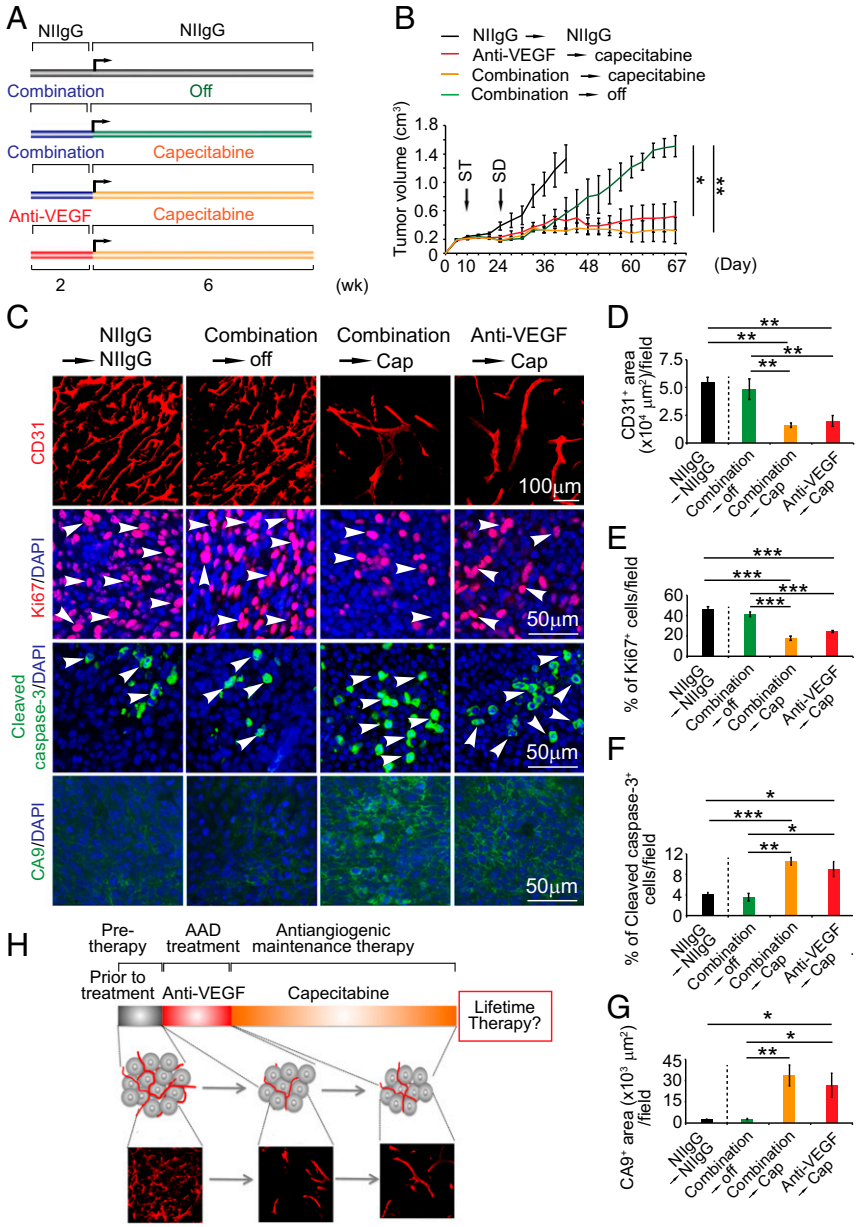

Fig. 7. Sustaining potent antitumor and antiangiogenic effects by an extremely low dose of capecitabine. (*A*) Sequential treatment schedule. (*B*) Growth rates of NIIgG-treated, VEGF blockade plus capecitabine switching to cessation-treated, VEGF blockade plus capecitabine switching to low-dose capecitabine-treated, and VEGF blockade switching to low-dose capecitabine-MC38 colorectal cancers (n = 6–9 mice per group). ST: starting treatment; SD: switching drug. (*C*) Representative histological images of CD31$^+$ blood vessels, Ki67$^+$ proliferating cells, cleaved caspase-3$^+$ apoptotic cells, and CA9$^+$ hypoxia. Arrowheads point to proliferating (red signal) and apoptotic (green signal) cells. (*D*–*G*) Quantifications of CD31$^+$ blood vessels, Ki67$^+$ proliferating cells, cleaved caspase-3$^+$ apoptotic cells, and CA9$^+$ hypoxia in various agent-treated tumors (n = 6–8 random fields per group). Data are means ± SEM. *P < 0.05; **P < 0.01; ***P < 0.001. NS, not significant. (*H*) Schematic diagram of capecitabine-based antiangiogenic maintenance therapy. Anti-VEGF treatment persists for a relatively short period (red bar), and the subsequent treatment was switched to an extremely low dose and nontoxic orally active capecitabine for long time. This therapeutic regimen produces robust antiangiogenic and antitumor effects.

long-term capecitabine therapy is the cumulative toxicity as described in other settings. Importantly, tumor microvessel density may serve as an independent and significant prognostic indicator for overall and relapse-free survival as seen in breast cancer patients (32). Thus, maintenance of low tumor vascular density by capecitabine would be important for improvement of cancer patient survivals. Upon withdrawal of AAD, capecitabine maintained the AAD-induced antiangiogenic effects for a long time without causing tumor revascularization. The antiangiogenic maintenance effects by capecitabine were virtually indistinguishable from the effects of receiving continuous AAD therapy. For antiangiogenic maintenance therapy, capecitabine is an ideal drug because (*i*) it is low cost (a daily cost of less than 10 US dollars per 75-kg patient using our low-dose antiangiogenic regimen); (*ii*) it has moderate side effects and toxicity; in our preclinical studies, we have not observed any obvious side effects caused by the low-dose capecitabine; (*iii*) it is an oral drug that can be conveniently administered to patients; and (*iv*) it is an existing FDA-approved drug for cancer therapy. Thus, capecitabine should be considered for antiangiogenic maintenance, especially aiming for lifetime therapy. Mechanistically, capecitabine may act as a broad-spectrum inhibitor of tumor angiogenesis by blocking multiple factor-triggered

signaling pathways. Through this broad action, the compensatory mechanism of drug resistance can be effectively blocked by capecitabine. Similarly, sequential therapy by anti-VEGF monotherapy such as bevacizumab followed by tyrosine kinase inhibitors (TKIs) that block multiple signaling pathways may also circumvent the anti-VEGF resistance. The rationale for this sequential treatment is that TKIs block non-VEGF–induced tumor angiogenesis. However, TKIs are often highly toxic and may not be appropriate for long-term therapy. This interesting issue warrants clinical validation.

Low-dose antiangiogenic chemotherapy (also called metronomic chemotherapy) has been suggested for treatment of cancer (33–36). Importantly, antiangiogenic scheduling of low-dose chemotherapy restores chemotherapy sensitivity in experimental resistant tumors (35). Despite the claims of their angiostatic activity, the antiangiogenic properties of various chemotherapeutics have not been systematically investigated. In fact, various chemotherapeutics possess different capacities for inhibition of tumor angiogenesis. If a nonantiangiogenic chemotherapeutic agent is chosen, it will not be able to sustain the anti-VEGF–triggered antiangiogenic effects. Based on the antiangiogenic activity of chemotherapeutics, the classical paradigm for selection of a chemotherapeutic drug for treatment of a particular cancer should be changed. The new paradigm would be that capecitabine should be used for antiangiogenic maintenance therapy for all cancer types. This concept will bring about paradigm shift during future clinical practice with chemotherapy. Taken together, we have identified an orally active, clinically available, and economically acceptable drug for long-term maintenance of the antiangiogenic effect in tumors. If validated in human cancer patients, this low-cost and nontoxic therapy will be beneficial for millions of cancer patients.

Materials and Methods

Cell Lines and Cell Culture. The mouse MC38 CRC cell line was kindly provided by Rubén Hernández at the Gene Therapy Unit, Center for Applied Medical Research, University of Navarra, Pamplona, Navarra, Spain. The human SW480 CRC cell line was purchased from the American Type Culture Collection (ATCC catalog no. CCL-228). The hTERT^{+}-BCE capillary endothelial cell line was isolated and generated as previously described (37). The human A549 nonsmall cell lung carcinoma cell line was kindly provided by Elias Arner at the Department of Medical Biochemistry and Biophysics, Karolinska Institutet, Stockholm, Sweden. The human HT29 CRC cell line and human MDA-MB-231 breast adenocarcinoma cell line were purchased from the ATCC (catalog no. HTB-26). HUVECs were kindly provided by Sonia Lain at the Department of Microbiology, Tumor and Cell Biology, Karolinska Institutet, Stockholm, Sweden. MC38, BCE, A549, HT29, and MDA-MB-231 cells were cultured in DMEM (HyClone; catalog no. SH30243.01) supplemented with 10% heat-inactivated FBS (HyClone; catalog no. SH30160.03), 100 U per mL penicillin, and 100 μg per mL streptomycin (HyClone; catalog no. SV30010). Human SW480 tumor cells were cultured in L-15 medium (Sigma-aldrich; catalog no. L1518-500 mL) supplemented with 10% heat-inactivated FBS (HyClone; catalog no. SH30160.03), 100 U/mL penicillin, and 100 μg/mL streptomycin. HUVECs were cultured in complete EGM-2 medium supplemented with heat-inactivated FBS (HyClone; catalog no. SH30160.03), 100 U/mL penicillin, and 100 μg/mL streptomycin (HyClone; catalog no. SV30010).

Endothelial Inhibition by Chemotherapeutics. Endothelial inhibition by chemotherapeutic drugs was determined by an MTT assay using the half maximal inhibitory concentration (IC_{50}) on capillary endothelial cells. Briefly, 5×10^3 capillary endothelial cells or tumor cells (A549, HT29, and MDA-MB-231) were seeded per well in a 96-well plate. After 72 h of incubation at various concentrations of 5-FU (Shanghai Xudong Haipu Pharmaceutical), gemcitabine (Jiangsu Haosen Pharmaceutical), pemetrexed (Qilu Pharmaceutical), cisplatin (Qilu Pharmaceutical), oxaliplatin (Jiangsu Hengrui Medicine), adriamycin (Shenzhen Wanle), paclitaxel (Hisun Pfizer Pharmaceuticals), docetaxel (Jiangsu Hengrui Medicine), or vinorelbine (Jiangsu Haosen Pharmaceutical), an MTT reagent (5 mg/mL; M5655; Sigma-Aldrich) was added to each well according to the manufacturer's protocol. Absorbance of densitometry at a 570-nm wavelength was measured by a spectrophotometer. For MC38, BCE, SW480, and HUVEC proliferation assays, a 48 h-MTT method was used. Briefly, 5–10 $\times 10^3$ cells were seeded in each well in a 96-well plate. Various concentrations of 5-FU were added to each well (triplicates were used for each concentration group). After 48 h incubation at 37 °C, absorbance of densitometry at the 570-nm wavelength was measured using a spectrophotometer. Data were presented as mean determinants of the optical density at 570 nm.

Animals. Female or male C57BL/6 mice at age 6–8 wk were provided by the Department of Microbiology, Tumor and Cell Biology animal facility at the Karolinska Institutet, Sweden, and housed in groups of 10 or fewer mice per cage. All animal studies were approved by the Northern Stockholm Animal Ethics Committee, and experiments were executed according to the guidelines of the ethical protocols.

Immunofluorescent Staining. Immunofluorescent staining of cultured cells was performed according to our previously described methods (38–40). Monolayers of MC38, BCE, SW480, and HUVEC cells were cultured to 80–90% confluence in a 10-cm^2 culture dish. Cells were grown at 40–60% confluence in each well in 12-well plates with a 15-mm diameter round cover glass (Thermo Fischer Scientific, catalog no. 174969). After 12 h of incubation, on the next day, 5-FU were added at various final concentrations of 0–2,500 ng/mL. After 48 h, cells were carefully washed twice with PBS and fixed for 10 min at room temperature with 100% methanol. Cells were washed twice with PBS, and nonspecific antigens were blocked with 4% normal goat serum (Vector Laboratories, catalog no. S-1000) for 30 min. Primary antibodies were incubated at 4 °C for overnight. A rat anti-mouse Ki67 (eBioscience, catalog no. SolA15, diluted 1:400 in PBS) and a rabbit anti-mouse cleaved caspase-3 (Cell Signaling, catalog no. 9961L, diluted 1:400 in PBS) were used. After rigorous washing, cells were incubated for 1 h at room temperature with secondary antibodies. A donkey anti-rat Alexa 488 (Thermo Fischer Scientific, catalog no. A21208, diluted 1:400) or a donkey anti-rabbit 488 (Thermo Fischer Scientific, catalog no. A21206, diluted 1:400) were used. Slides were washed twice with PBS and mounted with Vectashield (Vector laboratories, catalog no. H-1200). Images were taken with a fluorescent microscope (Nikon, ECLIPSE 90i). Quantification as a percentage of proliferating and apoptotic cells was done by Adobe Photoshop CS6 software with six to eight images per group.

Tumor Models and Treatment. Mouse MC38 CRC cells at a density of 1×10^6 or 3×10^6 cells were subcutaneously injected into the middorsal-back region of each mouse. Treatment was started when the tumor size reached around 0.2 cm^3. A humanized rabbit anti-mouse VEGF-neutralizing monoclonal antibody (BD0801) was used (13–15, 41) (Simcere Pharmaceutical). A rabbit NIIgG (catalog no. 10500C, Thermo Fischer Scientific) was used as a control. Anti-VEGF antibody and NIIgG were intraperitoneally injected twice per week at 5 mg/kg into each mouse. After treatments with anti-VEGF and NIIgG, 5-FU or capecitabine (Roche) treatment was started daily by i.p. injection or oral gavage, respectively.

Blood Sample, Liver Function, and Kidney Function Tests. Blood was immediately collected from the right ventricle after the mice were killed. Hematological parameters including red blood cell count and white blood cell count were analyzed by an auto-hematology analyzer (Mindray, catalog no. BC-2800Vet) (42). Serum and plasma were prepared in the presence or absence of the anticoagulant EDTA, respectively, followed by centrifugation at 2,000 $\times$ *g* for 30 min. Liver functions were analyzed by blood albumin, ALT, and AST using the following biochemistry kits from Huili Biotech: albumin (catalog no. K509), ALT (catalog no. K048b), and AST (catalog no. K049a). Assay procedures were followed according to the manufacturer's instruction. Kidney functions were analyzed by blood creatinine and urea nitrogen levels using the following biochemistry kits from Huili Biotech: creatinine (catalog no. K006) and urea nitrogen (catalog no. K072b). Assay procedures were followed according to the manufacturer's instruction.

Immunohistochemistry and Whole-Mount Staining. Paraffin-embedded tissues were cut into 5-μm thickness, mounted on glass slides, deparaffinized in Tissue-Clear (catalog no. 1466, Sakura), and sequentially rehydrated with 99, 95, and 70% ethanol. Antigen retrieval was done in a low-pH buffer (Vector Laboratories, catalog no. H3300). After 5 min of preheating, samples were heated in a microwave for 20 min. After antigen retrieval, samples were washed twice with PBS and blocked for 30 min at room temperature with 4% normal goat serum. A rat anti-mouse Ki67 (eBioscience, catalog no. SolA15), a rabbit anti-mouse cleaved caspase-3 (Cell Signaling, catalog no. 9961L), and a rabbit anti-mouse CA9 antibody (Novus Biologicals, catalog no. NB100-417), all diluted at 1:400 in PBS, were applied to the samples and incubated at 4 °C overnight. After rigorous washing with PBS, an Alexa 488-conjugated donkey anti-rat (Thermo Fischer Scientific, catalog no. A21208, diluted 1:400) and an Alexa

488-conjugated donkey anti-rabbit (Thermo Fischer Scientific, catalog no. A21206, diluted 1:400) were used as secondary antibodies. Secondary antibodies were incubated at room temperature for 40 min. Slides were washed with PBS for two times and mounted with Vectashield (catalog no. H1200).

Whole-mount staining was performed using our standard protocol (43–47). Briefly, tissues were cut into small pieces, and thin slices were fixed in 4% PFA overnight, followed by treatment with proteinase K (20 μg/mL). Tissues were incubated overnight at 4 °C with a goat anti-mouse CD31 antibody (catalog no. AF3628, R&D). After washing, tissue samples were further stained for 2 h at room temperature with a secondary antibody to recognize the primary antibody: a donkey anti-goat Alexa 555 antibody (catalog no. A21432, Invitrogen). After thorough washing, slides were mounted with Vectashield (catalog no. H1200) and examined under a confocal microscope (Zeiss Confocal LSM510 Microscope). Three-dimensional images of each tissue sample were projected and quantitatively analyzed from at least eight random fields using an Adobe Photoshop CS6 software program.

Blood Perfusion and Vascular Permeability. At the experimental endpoints after treatment, each mouse was anesthetized and intravenously injected with 100 μL of 2,000 kDa of lectin (Vector Laboratories, catalog no. FL-1081). Animals were killed 5 min after lectin injection, and tissues were dissected and immediately fixed at 4 °C with 4% PFA. For permeability assay, 100 μL of 70 kDa of lysinated fluorescein-labeled dextran (catalog no. D1818, Invitrogen) was intravenously injected into each mouse. Animals were killed 15 min after dextran injection. Tumor tissues were carefully dissected, whole-mount-stained, and examined by confocal microscopy.

Statistical Analysis. A standard two-tailed Student's *t* test was used for all statistical analyses. All sample sizes were appropriate for assumption of normal distribution, and variance was similar between compared groups. The statistical values of $P < 0.05$, $P < 0.01$, and $P < 0.001$ were considered statistically significant. Values of mean determinants are presented as ± SEM.

ACKNOWLEDGMENTS. The Y.C. laboratory is supported through research grants from the European Research Council Advanced Grant ANGIOFAT (Project no. 250021); the Swedish Research Council; the Swedish Cancer Foundation; the Children Cancer Foundation; the Diabetes Foundation; the Karolinska Institute Foundation; the Karolinska Institute Distinguished Professor Award; the Torsten Soderbergs Foundation; the Maud and Birger Gustavsson Foundation; the NOVO Nordisk Foundation; and the Knut and Alice Wallenberg Foundation. Guohui Nie is supported by Fund for High Level University Construction of Medical Discipline (2016031638), China and The Shenzhen Science and Technology Innovation Committee (JCYJ20150403091443336).

1. Folkman J (1971) Tumor angiogenesis: Therapeutic implications. *N Engl J Med* 285: 1182–1186.
2. Cao Y, et al. (2011) Forty-year journey of angiogenesis translational research. *Sci Transl Med* 3:114rv3.
3. Ferrara N, Adamis AP (2016) Ten years of anti-vascular endothelial growth factor therapy. *Nat Rev Drug Discov* 15:385–403.
4. Wadzinski MG, et al. (1987) Heparin-binding angiogenesis factors: Detection by immunological methods. *Clin Physiol Biochem* 5:200–209.
5. Davis S, et al. (1996) Isolation of angiopoietin-1, a ligand for the TIE2 receptor, by secretion-trap expression cloning. *Cell* 87:1161–1169.
6. Maisonpierre PC, et al. (1997) Angiopoietin-2, a natural antagonist for Tie2 that disrupts in vivo angiogenesis. *Science* 277:55–60.
7. Folkman J (2007) Angiogenesis: An organizing principle for drug discovery? *Nat Rev Drug Discov* 6:273–286.
8. Cao Y (2009) Positive and negative modulation of angiogenesis by VEGFR1 ligands. *Sci Signal* 2:re1.
9. Shibuya M (2014) VEGF-VEGFR signals in health and disease. *Biomol Ther (Seoul)* 22: 1–9.
10. Ferrara N, Gerber HP, LeCouter J (2003) The biology of VEGF and its receptors. *Nat Med* 9:669–676.
11. Cao Y (2014) VEGF-targeted cancer therapeutics-paradoxical effects in endocrine organs. *Nat Rev Endocrinol* 10:530–539.
12. Kamba T, et al. (2006) VEGF-dependent plasticity of fenestrated capillaries in the normal adult microvasculature. *Am J Physiol Heart Circ Physiol* 290:H560–H576.
13. Yang Y, et al. (2016) Discontinuation of anti-VEGF cancer therapy promotes metastasis through a liver revascularization mechanism. *Nat Commun* 7:12680.
14. Zhang Y, et al. (2016) Endocrine vasculatures are preferable targets of an antitumor ineffective low dose of anti-VEGF therapy. *Proc Natl Acad Sci USA* 113:4158–4163.
15. Yang Y, et al. (2013) Anti-VEGF- and anti-VEGF receptor-induced vascular alteration in mouse healthy tissues. *Proc Natl Acad Sci USA* 110:12018–12023.
16. Kerbel RS (2008) Tumor angiogenesis. *N Engl J Med* 358:2039–2049.
17. Kim KJ, et al. (1993) Inhibition of vascular endothelial growth factor-induced angiogenesis suppresses tumour growth in vivo. *Nature* 362:841–844.
18. Hurwitz H, et al. (2004) Bevacizumab plus irinotecan, fluorouracil, and leucovorin for metastatic colorectal cancer. *N Engl J Med* 350:2335–2342.
19. Perren TJ, et al.; ICON7 Investigators (2011) A phase 3 trial of bevacizumab in ovarian cancer. *N Engl J Med* 365:2484–2496.
20. Sandler A, et al. (2006) Paclitaxel-carboplatin alone or with bevacizumab for non-small-cell lung cancer. *N Engl J Med* 355:2542–2550.
21. Bruce JY, et al. (2014) A phase I pharmacodynamic trial of sequential sunitinib with bevacizumab in patients with renal cell carcinoma and other advanced solid malignancies. *Cancer Chemother Pharmacol* 73:485–493.
22. Haemmerle M, et al. (2016) FAK regulates platelet extravasation and tumor growth after antiangiogenic therapy withdrawal. *J Clin Invest* 126:1885–1896.
23. Powles T, et al. (2013) A prospective evaluation of VEGF-targeted treatment cessation in metastatic clear cell renal cancer. *Ann Oncol* 24:2098–2103.
24. Kuczynski EA, et al. (2016) Co-option of liver vessels and not sprouting angiogenesis drives acquired sorafenib resistance in hepatocellular carcinoma. *J Natl Cancer Inst* 108:djw030.
25. Allegra CJ, et al. (2011) Phase III trial assessing bevacizumab in stages II and III carcinoma of the colon: Results of NSABP protocol C-08. *J Clin Oncol* 29:11–16.
26. Allegra CJ, et al. (2013) Bevacizumab in stage II-III colon cancer: 5-Year update of the National Surgical Adjuvant Breast and Bowel Project C-08 trial. *J Clin Oncol* 31: 359–364.
27. de Gramont A, et al. (2012) Bevacizumab plus oxaliplatin-based chemotherapy as adjuvant treatment for colon cancer (AVANT): A phase 3 randomised controlled trial. *Lancet Oncol* 13:1225–1233.
28. Mancuso MR, et al. (2006) Rapid vascular regrowth in tumors after reversal of VEGF inhibition. *J Clin Invest* 116:2610–2621.
29. Arbiser JL, Arbiser ZK, Majzoub JA (1993) Effects of hydroxyurea and cyclic adenosine monophosphate/protein kinase A inhibitors on the expression of the human chorionic gonadotropin alpha subunit and c-myc genes in choriocarcinoma. *J Endocrinol Invest* 16:849–856.
30. Arbiser JL, Arbiser ZK, Majzoub JA (1993) Differential regulation of choriocarcinoma gene expression by DNA synthesis inhibitors. *Endocr J* 40:263–268.
31. Arbiser JL, Arbiser ZK, Majzoub JA (1991) Regulation of gene expression in choriocarcinoma by methotrexate and hydroxyurea. *Endocrinology* 128:972–978.
32. Weidner N, et al. (1992) Tumor angiogenesis: A new significant and independent prognostic indicator in early-stage breast carcinoma. *J Natl Cancer Inst* 84:1875–1887.
33. Gately S, Kerbel R (2001) Antiangiogenic scheduling of lower dose cancer chemotherapy. *Cancer J* 7:427–436.
34. Kerbel RS, Klement G, Pritchard KI, Kamen B (2002) Continuous low-dose anti-angiogenic/metronomic chemotherapy: From the research laboratory into the oncology clinic. *Ann Oncol* 13:12–15.
35. Browder T, et al. (2000) Antiangiogenic scheduling of chemotherapy improves efficacy against experimental drug-resistant cancer. *Cancer Res* 60:1878–1886.
36. Gasparini G (2001) Metronomic scheduling: The future of chemotherapy? *Lancet Oncol* 2:733–740.
37. Veitonmäki N, et al. (2003) Immortalization of bovine capillary endothelial cells by hTERT alone involves inactivation of endogenous p16INK4A/pRb. *FASEB J* 17:764–766.
38. Cao Y, et al. (1998) Vascular endothelial growth factor C induces angiogenesis in vivo. *Proc Natl Acad Sci USA* 95:14389–14394.
39. Cao R, et al. (2012) Collaborative interplay between FGF-2 and VEGF-C promotes lymphangiogenesis and metastasis. *Proc Natl Acad Sci USA* 109:15894–15899.
40. Ji H, et al. (2014) TNFR1 mediates TNF-α-induced tumour lymphangiogenesis and metastasis by modulating VEGF-C-VEGFR3 signalling. *Nat Commun* 5:4944.
41. Seki T, et al. (2016) Endothelial PDGF-CC regulates angiogenesis-dependent thermogenesis in beige fat. *Nat Commun* 7:12152.
42. Xue Y, et al. (2011) PDGF-BB modulates hematopoiesis and tumor angiogenesis by inducing erythropoietin production in stromal cells. *Nat Med* 18:100–110.
43. Honek J, et al. (2014) Modulation of age-related insulin sensitivity by VEGF-dependent vascular plasticity in adipose tissues. *Proc Natl Acad Sci USA* 111: 14906–14911.
44. Hosaka K, et al. (2013) Tumour PDGF-BB expression levels determine dual effects of anti-PDGF drugs on vascular remodelling and metastasis. *Nat Commun* 4:2129.
45. Iwamoto H, et al. (2015) PlGF-induced VEGFR1-dependent vascular remodeling determines opposing antitumor effects and drug resistance to Dll4-Notch inhibitors. *Sci Adv* 1:e1400244.
46. Lim S, et al. (2012) Cold-induced activation of brown adipose tissue and adipose angiogenesis in mice. *Nat Protoc* 7:606–615.
47. Lim S, et al. (2014) VEGFR2-mediated vascular dilation as a mechanism of VEGF-induced anemia and bone marrow cell mobilization. *Cell Reports* 9:569–580.